NANO LETTERS

Letter

pubs.acs.org/NanoLett

3D Printed Quantum Dot Light-Emitting Diodes

Yong Lin Kong,[†] Ian A. Tamargo,[‡] Hyoungsoo Kim,[†] Blake N. Johnson,[†] Maneesh K. Gupta,[†] Tae-Wook Koh,[§] Huai-An Chin,[§] Daniel A. Steingart,[†,⊥] Barry P. Rand,[§,⊥] and Michael C. McAlpine*[,†]

[†]Department of Mechanical and Aerospace Engineering, Princeton University, Princeton, New Jersey 08544, United States

[‡]Department of Chemistry, Princeton University, Princeton, New Jersey 08544, United States

[§]Department of Electrical Engineering, Princeton University, Princeton, New Jersey 08544, United States

[⊥]Andlinger Center for Energy and the Environment, Princeton University, Princeton, New Jersey 08544, United States

Supporting Information

ABSTRACT: Developing the ability to 3D print various classes of materials possessing distinct properties could enable the freeform generation of active electronics in unique functional, interwoven architectures. Achieving seamless integration of diverse materials with 3D printing is a significant challenge that requires overcoming discrepancies in material properties in addition to ensuring that all the materials are compatible with the 3D printing process. To date, 3D printing has been limited to specific plastics, passive conductors, and a few biological materials. Here, we show that diverse classes of materials can be 3D printed and fully integrated into device components with active properties. Specifically, we demonstrate the seamless interweaving of five different materials, including (1) emissive semiconducting inorganic nanoparticles, (2) an elastomeric matrix, (3) organic polymers as charge transport layers, (4) solid and liquid metal leads, and (5) a UV-adhesive transparent substrate layer. As a proof of concept for demonstrating the integrated functionality of these materials, we 3D printed quantum dot-based light-emitting diodes (QD-LEDs) that exhibit pure and tunable color emission properties. By further incorporating the 3D scanning of surface topologies, we demonstrate the ability to conformally print devices onto curvilinear surfaces, such as contact lenses. Finally, we show that novel architectures that are not easily accessed using standard microfabrication techniques can be constructed, by 3D printing a 2 × 2 × 2 cube of encapsulated LEDs, in which every component of the cube and electronics are 3D printed. Overall, these results suggest that 3D printing is more versatile than has been demonstrated to date and is capable of integrating many distinct classes of materials.

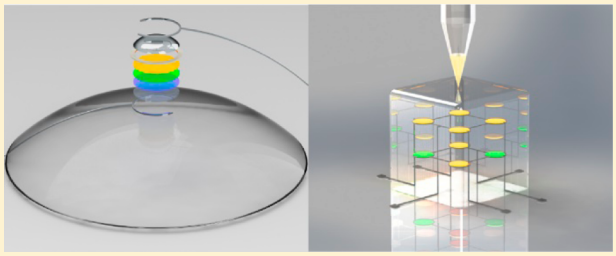

KEYWORDS: *3D printing, quantum dot light-emitting devices, hybrid materials integration, interwoven electronics, additive manufacturing*

The freeform generation of active electronics in unique architectures that transcend the planarity inherent to conventional microfabrication techniques has been an area of increasing scientific interest.[1−9] Three-dimensional large-scale integration (3D-LSI) can reduce the overall footprint and power consumption of electronics and is usually accomplished via stacks of two-dimensional semiconductor wafers, in which interconnects between layers are achieved using wire-bonding[10] or through-silicon vias.[11] Overcoming this "2D barrier" has significant potential application beyond improving the scalability in semiconductor integration technologies. For instance, the ability to seamlessly incorporate electronics into three-dimensional constructs could impart functionalities to biological[12,13] and mechanical[14,15] systems, such as advanced optical, computation, or sensing capabilities. For example, integration of electronics on otherwise passive structural medical instruments such as catheters,[16] gloves,[17] and contact lenses[18,19] are critical for next generation applications such as real-time monitoring of physiological conditions. Such integration has been previously demonstrated via meticulous transfer printing of prefabricated electronics[3,20,21] or interfacing materials[22] via dissolvable media such as silk[22,23] on nonplanar surface topologies. An alternative approach is to attempt to interweave electronics in three dimensions from the bottom up. Yet, attaining seamless interweaving of electronics is challenging due to the inherent material incompatibilities and geometrical constraints of traditional microfabrication processing techniques.

This hybrid integration has been accomplished via a number of novel and creative strategies that involve various approaches for assembling prefabricated electronic components into three-dimensional structures. For instance, the "click-e-bricks" method has achieved integration via the creation of elastomeric bricks, which can then be coassembled with electrical components into active composite structures.[24] In addition,

Received: August 29, 2014
Revised: October 15, 2014
Published: October 31, 2014

nanomaterials such as nanowires can be vertically stacked into three-dimensional field-effect transistors via layer-by-layer assembly.[25] The repeated transfer of nanomaterials with elastomeric stamps has also been used to create heterogeneously integrated electronic systems with three-dimensional layouts.[2] Macroporous three-dimensional nanoelectronic networks have also been prepared from ordered two-dimensional nanowires that are fabricated with conventional lithography, which enable three-dimensional interpenetration with host materials.[7] Most intriguingly, three-dimensional electrical devices have also been demonstrated via self-assembly processes.[26] The self-assembly of prefabricated chips into three-dimensional heterogeneous electronic systems can be driven by surface tension,[27] capillary interaction,[28] or by biomimicking protein folding.[29]

Extrusion-based 3D printing is an additive manufacturing technique that represents an alternative approach, offering freeform fabrication capabilities.[13,30−34] This is enabled by slicing a 3D computer-aided design (CAD) model to generate new geometrical form factors in a layer-by-layer fashion. Yet, to date, the 3D printing of electronic components has been limited to the printing of batteries,[35] strain sensors,[36] interdigitated-electrode capacitors,[37] and passive metallic structures such as interconnects[38] and antennas on surfaces[15] or within biological organs.[13] The ability to directly incorporate materials with a range of diverse functionalities is particularly attractive as it could allow the simultaneous, comprehensive, and direct printing of structural, biological, and electronic materials that capture the complete spectra of material properties.[39−41] At the fundamental level, 3D printing should be entirely capable of creating spatially heterogeneous multimaterial structures by dispensing a wide range of material classes with disparate viscosities[14] and functionalities, including semiconducting colloidal nanomaterials,[42−44] elastomeric matrices,[36] organic polymers,[45] and liquid[46−48] and solid metals.[4,15] Compared to traditional microfabrication techniques, the exclusion of harsh chemicals or high temperature processing could enable the direct integration of active electrical components with unique mechanical architectures and within biological constructs,[13,31] but without the requirement of separate assembly steps.

Here, we show that 3D printing can achieve diverse multimaterial integration to create active semiconducting electronic devices. Our approach consists of three key steps. First, it identifies electrodes, semiconductors, and polymers that possess desired functionalities and exist in printable formats. Next, care is taken to ensure that these materials are dissolved in orthogonal solvents so as not to compromise the integrity of the underlying layers during the layer-by-layer printing process.[41] Finally, the interwoven patterning of these materials is achieved via direct dispensing in a CAD-designed construct.

As a proof of concept of this approach, here, we present the first fully 3D extrusion-printed semiconducting quantum dot light-emitting diodes (QD-LEDs), as represented in Figure 1A. Nanoelectronics such as QD-LEDs possess a number of interesting properties. First, the emission wavelength is tunable simply by changing the size of the quantum dots (QDs).[49] Second, the ability to synthesize highly monodisperse QDs with narrow size distributions leads to narrow emission spectra.[50] Third, QDs are significantly smaller than the optical wavelength, leading to negligible scattering losses.[51] Inspired by previously published all-solution-processed QD-LEDs,[41,52,53] we designed the 3D printed QD-LEDs with the following

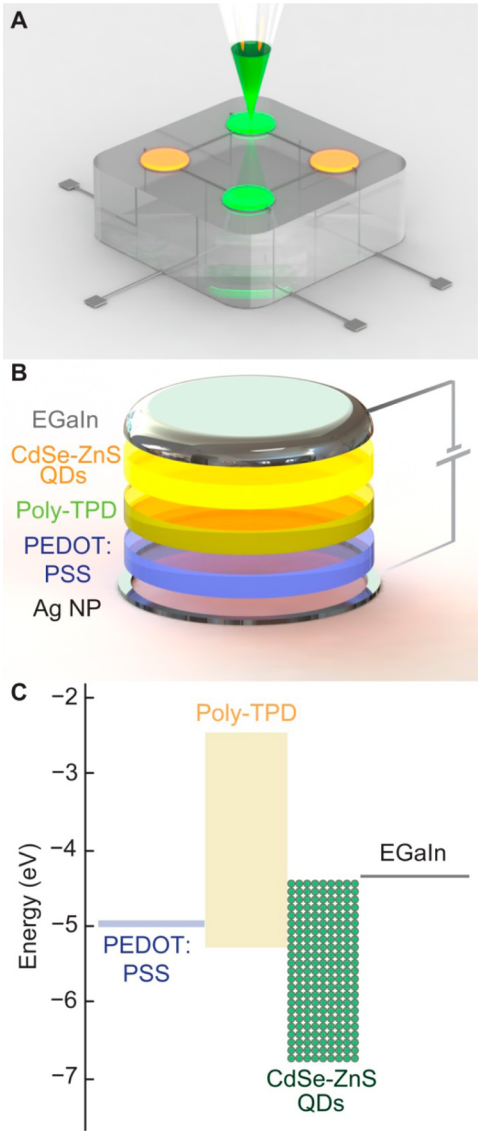

Figure 1. 3D printed QD-LEDs. (A) Direct 3D printing of QD-LEDs on a substrate. (B) Layer-by-layer schematic of the various QD-LED components. (C) QD-LED energy level diagram.

layers: (1) cadmium selenide/zinc sulfide (CdSe/ZnS) core−shell QDs as the emission layer, (2) poly[*N*,*N*′-bis(4-butylphenyl)-*N*,*N*′-bis(phenyl)-benzidine] (poly-TPD) as the hole transport layer, (3) poly(ethylenedioxythiophene):polystyrene sulfonate (PEDOT:PSS) as the transparent anode, surrounded by (4) a sintered silver nanoparticle (AgNP) ring metallic interconnect, and (5) a eutectic gallium indium liquid metal (EGaIn) cathode. These various layers are shown in Figure 1B. A schematic energy level diagram of the designed structure is shown in Figure 1C (using literature values),[41,54] in which holes are injected from PEDOT:PSS into the QDs through poly-TPD[41,44] and electrons are injected directly from EGaIn into the QDs.

We first examined the printing of the hole transport layer on PEDOT:PSS, which is directly adjacent to the QD layer (see Supporting Information). Poly-TPD exhibits strong intrinsic resistance to nonpolar solvents after annealing.[41] Further, it has a luminescence efficiency that is significantly lower than QDs, which minimizes the residual organic emission and preserves the color purity of the QD-LED output.[55] Next, the most

dx.doi.org/10.1021/nl5033292 | *Nano Lett.* 2014, 14, 7017−7023

critical component is optimizing the printing of the semiconducting CdSe/ZnS QD emissive layer. 3D printing may have an advantage in this regard, as spin coating[41] of QDs wastes 94−97% of the starting solution,[56] which is associated with a 20-fold increase in QD material cost.[57] Yet, uniform printing of the QDs must be achieved for reliable device behavior. We exploited solutal Marangoni effects,[58] which suppress the accumulation of suspended particles in a drying droplet of solution near the pinned contact line that is due to the capillary flow, that is, the so-called coffee ring pattern.[59] The Marangoni effect is known to be due to the different surface tensions associated with the two liquid components of a binary mixture, which create a solutal Marangoni flow. Under optimal conditions, the particles may deposit in a self-assembled uniform layer.[60] We prepared the CdSe/ZnS QDs in a binary mixture of toluene and dichlorobenzene and investigated the uniformity of the printed QD layer on the poly-TPD surface by varying the mixing ratio of the two liquids (temperature = 23.5 ± 0.5 °C and relative humidity = 22.5 ± 1%).

Figure 2A shows that for the pure toluene case, the contact line recedes as evaporation occurs (see Supporting Information Movie 1). Therefore, most QDs are concentrated in a small region near the droplet center and distributed over a significantly smaller region than the target area, which is represented by the green dashed circle line. Further characterization by profilometry shows a maximum height of 5.6 μm at the receded coffee ring and low uniformity of the QD layer as indicated by a root-mean-square roughness value (R_{RMS}) of 900 nm at the inner circular region. Note that the R_{RMS} value was measured in the direction shown by the green arrow from 1 mm to 3 mm at the x axis in Figure 2A. This lack of uniformity in the printed QDs causes significant difficulties in subsequent printing steps, reducing device performance and yield. Figure 2B shows the results from a binary mixture of 80% toluene and 20% dichlorobenzene (see Supporting Information Movie 2). This mixture allows the contact line to remain pinned everywhere, resulting in the formation of a more uniformly distributed QD layer, except at the outer region of the contact line. For example, at the same 1 mm radius region, the profilometer measurement shows a maximum height of only 260 nm and R_{RMS} of 110 nm. The annular ring pattern deposition observed is due to the stick-and-slip mode of the contact line movement.[61,62] Finally, Figure 2C shows that further increasing the dichlorobenzene concentration does not improve QD layer uniformity (see Supporting Information Movie 3), suggesting that the 80/20 v/v mixture of toluene/dichlorobenzene is the optimal ratio for printing the QDs.

As shown in Figure 1B, the QD-LED also contains an underlying anode and a AgNP metallic interconnect as a conductive pathway in addition to the QD emissive layer and the poly-TPD hole transport layer. A transparent and highly conductive surface was created by printing PEDOT:PSS formulated in diethylene glycol and ethanol.[63] The conductive ring comprised of synthesized AgNPs was also printed surrounding the PEDOT:PSS film. As shown in the Supporting Information, the porous and hydrophilic nature of the printed AgNP structure enables good electrical contact with the printed PEDOT:PSS and defines a boundary for the PEDOT:PSS ink. The EGaIn[47,48] cathode is nontoxic, highly conductive (3.4×10^4 S cm^{-1}), and has a work function of −4.3 eV.[54] As shown in Figure 1C, the work function is well aligned with the electron affinity of the adjacent CdSe-ZnS QDs, enabling electron

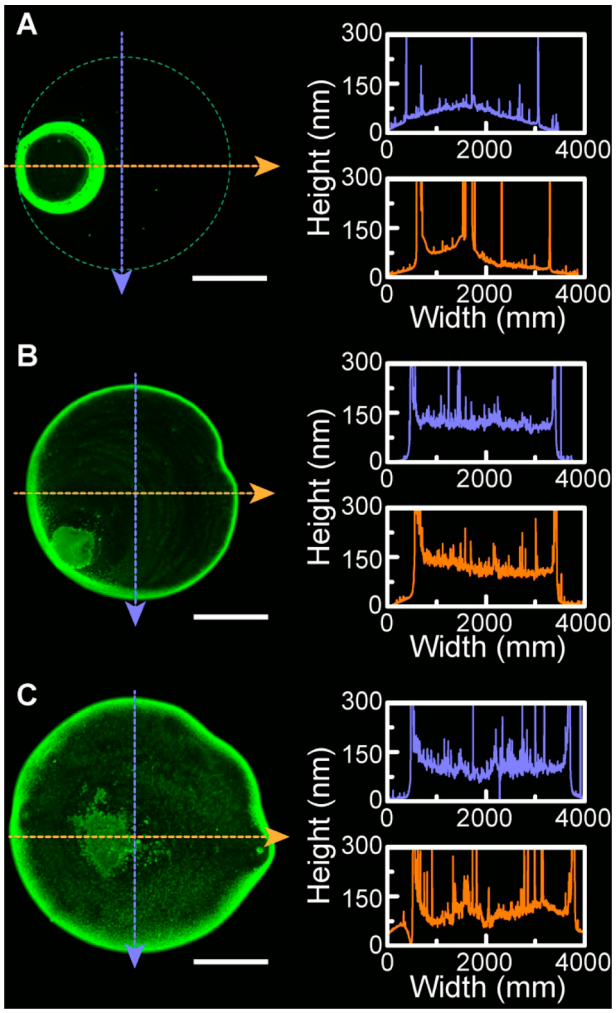

Figure 2. Analysis of binary solvent mixtures for uniform deposition of colloidal CdSe/ZnS QDs on poly-TPD, with increasing volume fractions of (A) 0%, (B) 20%, and (C) 50%, dichlorobenzene in toluene. The green dashed line indicates the initial droplet deposition area. The graphs show profilometry measurements of the QDs along the two perpendicular directions (blue, vertical; orange, horizontal). Scale bars are 1 mm.

injection into the QD layers without an electron transport layer, simplifying the QD-LED structure. The EGaIn can be printed directly at room temperature (melting point = 15.5 °C) and forms mechanically stable 3D structures due to the formation of a thin oxide layer at the surface of the liquid.[46,64] Most importantly, EGaIn does not require heat treatment for sintering and forms conformal physical contact with the QD layer without releasing any solvents.[48] The dispensed EGaIn is then vertically connected with room-temperature-vulcanized conductive Ag microparticle-infused silicone rubber and encapsulated in a printed insulating acrylate-based UV adhesive.

Having established printing strategies for the five different device layers, we next examined the performance of fully printed QD-LEDs to confirm that the printed layers were electronically active and functional. We emphasize that all QD-LED layers and components were 3D printed in these devices, in contrast to other efforts in which only the QD layer was printed.[56,65−68] To demonstrate the color tunability of the QD-LED emission, we printed green (550 nm) and orange-red (618 nm) QD-LEDs. As shown in Figure 3A and B, respectively, the

dx.doi.org/10.1021/nl5033292 | Nano Lett. 2014, 14, 7017−7023

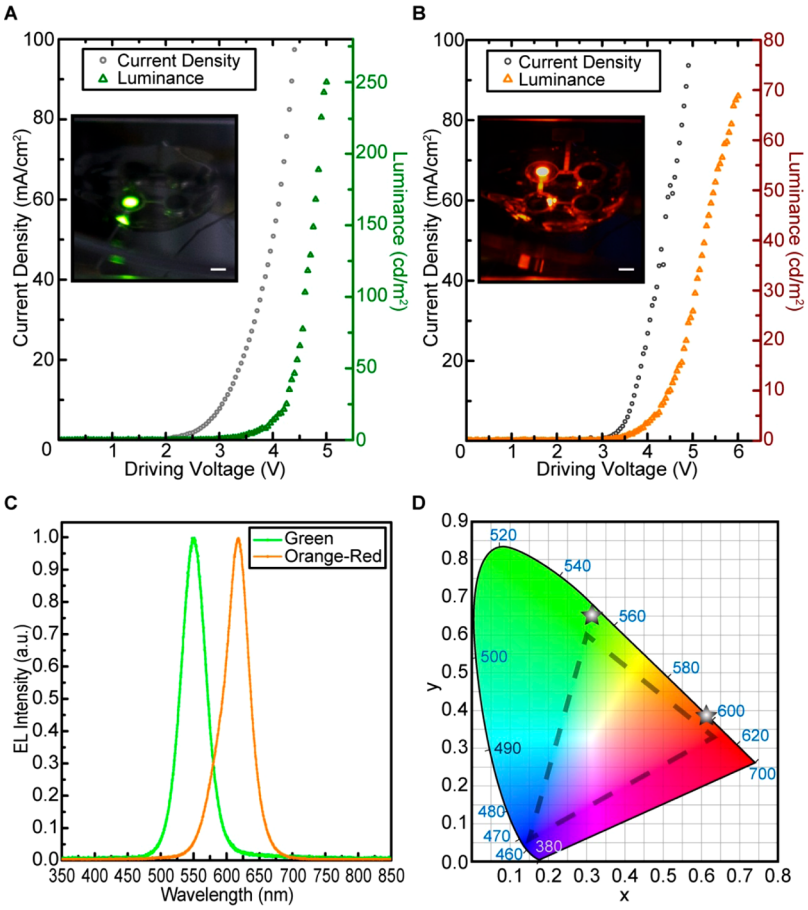

Figure 3. Performance of 3D printed QD-LEDs. Current density−voltage curves and forward luminance output of printed (A) green and (B) orange-red QD-LEDs. Insets show the electroluminescence (EL) output from the QD-LEDs. Scale bars are 2 mm. (C) Normalized EL spectra with peak emission intensities from green and orange-red QD-LEDs. (D) Color coordinates of the green (0.323, 0.652) and orange-red (0.612, 0.383) QD-LEDs, indicated by stars on the Commission International de l'Eclairage (CIE) 1931 chromaticity diagram. Dashed lines indicate the saturation windows for a high definition television color standard by the National Television System Committee. (The background of the CIE diagram is adapted from CIExy1931.svg of Wikimedia Commons.)

green QD-LED achieved a maximum brightness of 250 cd/m^2 at 5 V, whereas the orange-red QD-LED achieved a maximum brightness of 70 cd/m^2 at 8 V. The fully printed green QD-LED structure emits 100 cd/m^2 at 4.5 V, which compares favorably to a 9.3 V requirement for that brightness level in direct-current driven inkjet-printed QD-LEDs[56,68] or 12.2 V for mist-coated QD-LEDs.[67] Green QD-LEDs deposited via transfer printing[66] and spin-coating[41] have been shown to achieve 2300 cd/m^2 and 24 000 cd/m^2 at 5 V, respectively. Thus, significant improvements in the performance of the 3D printed QD-LEDs will be possible by controlling layer thickness and uniformity, experimenting with ink formulations, processing optimizations, and introducing an inert printing environment. Further, as shown in the electroluminescence spectra in Figure 3C, the printed devices exhibited pure color emission from the QD emissive layer with a narrow full-width at half-maxima (fwhm) of 43 nm for both colors. This is on par with the color purity from QD-LEDs made with established methods.[39,41] Figure 3D quantifies the color quality based on a chromaticity diagram that maps the range of physically produced colors to an objective description of color sensations by the average human.[39,57] As indicated by the green (0.323, 0.652) and orange-red (0.612, 0.383) Commission International de l'Eclairage (CIE) 1931 chromaticity coordinates in Figure 3D, the printed QD-LEDs generate highly saturated color emissions, which could enable the creation of displays that can subtend the color gamut at levels greater than the high-definition television standard (dashed line triangle).[39] We note that devices using AgNPs as the cathode were also examined and provided brightness values up to 11 cd/m^2 at 13 V (Supporting Information).

This 3D printing-based approach allowed for the direct printing of QD-LEDs on polyimide tape and subsequent transfer to a variety of surfaces, including polycarbonate, nitrile gloves, and paper (Supporting Information). In addition to glass substrates, we have also investigated the printing of QD-LEDs on various transparent and printable materials, including UV adhesives, poly(vinyl alcohol), and polydimethylsiloxane (Supporting Information).

The development of 3D printing techniques has been accompanied by the codevelopment of 3D scanning technologies. This suggests a means for conformally printing on nonplanar objects that may be achieved by first scanning the geometry of the object, incorporating the precise topography into a CAD program, and finally adjusting the printing process to precisely match the underlying shape. To impart conformal printing capabilities to our 3D printing-based fabrication approach, we integrated 3D structured-light scanning to generate a compatible computer model of the target surface geometry, which in turn served as the substrate template.[69−71]

dx.doi.org/10.1021/nl5033292 | Nano Lett. 2014, 14, 7017−7023

This integrated scanning and printing approach allows for the intimate and conformal printing of electronics on nonflat surfaces.[3,23,72] As a proof of concept, QD-LEDs were printed directly on a contact lens, whose geometry was first 3D scanned to calibrate the printing to its precise topography (Figure 4A).

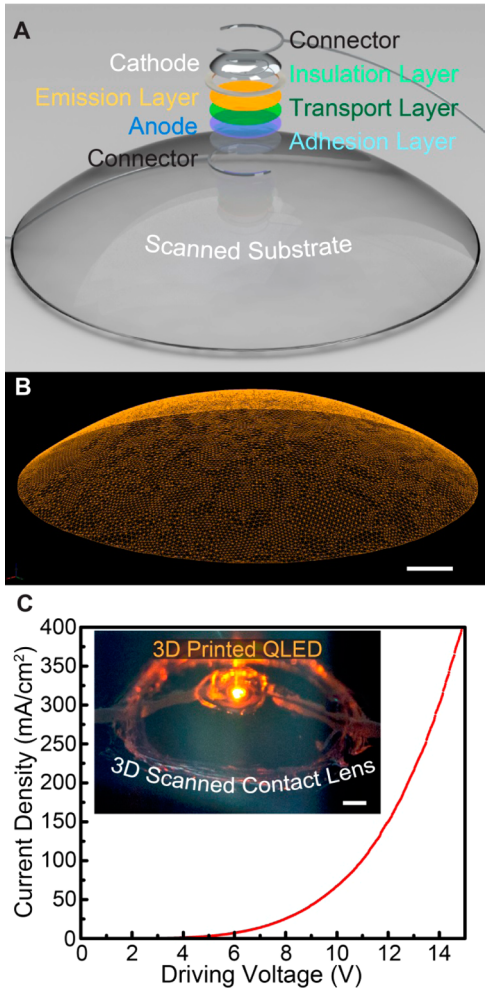

Figure 4. 3D printed QD-LED on a 3D scanned onto a curvilinear substrate. (A) CAD model showing the QD-LED components and conformal integration onto a curvilinear substrate. (B) 3D model of a contact lens acquired by 3D structured-light scanning. (C) Current density vs voltage characteristics of the 3D printed QD-LEDs on top of the 3D scanned contact lens. The inset shows the electroluminescence output from the printed QD-LED. Scale bars are 1 mm.

This can then be conformally merged with the QD-LED electronic components using 3D CAD software. The scan data are shown in Figure 4B, which provides a mesh representation of the surface of the contact lens. The inset of Figure 4C shows the electroluminescence from an orange-red QD-LED that was printed on the 3D scanned contact lens. The electrical performance is shown in Figure 4C. Critically, despite the significant roughness of the UV adhesive (Supporting Information), the electrical performance does not suffer significantly as compared to the controlled planar substrate conditions shown in Figure 3B. We envision that the direct printing of QD-LEDs on contact lenses can potentially be used for wearable displays[19] or continuous on-eye glucose sensors.[18,73]

A key advantage of 3D printing is the ability to fabricate devices and architectures from the ground up in a layer-by-layer process, which suggests that active electronics which are interwoven within biological and encapsulating materials are achievable.[13,36] As a proof of concept of this approach, we tested the ability to generate multidimensional electronic arrays of interconnected QD-LEDs. The concept is shown in Figure 5A, consisting of a multicolor, embedded, 2 × 2 × 2 matrix

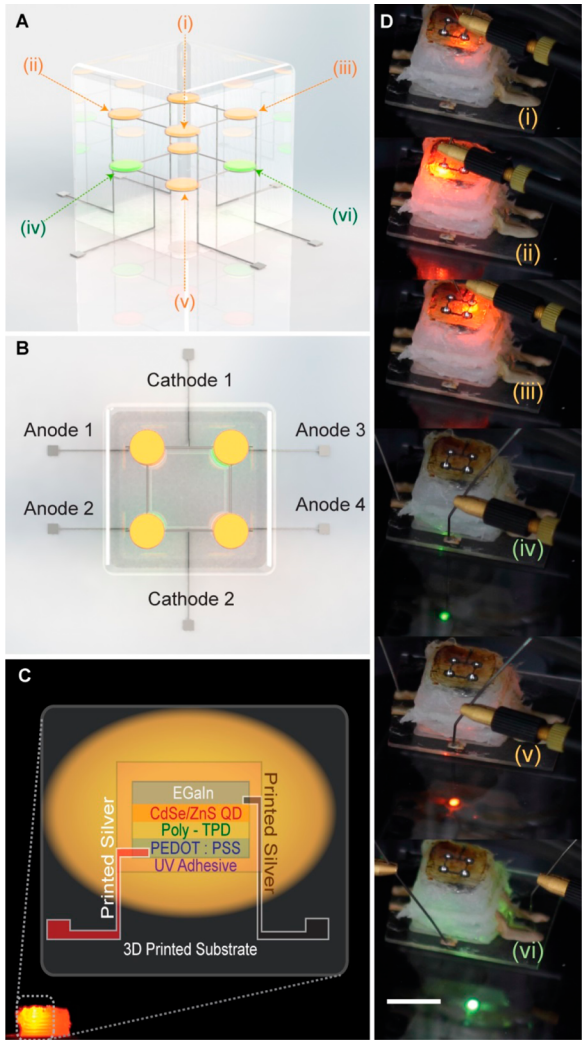

Figure 5. 3D printed 2 × 2 × 2 multidimensional array of embedded QD-LEDs. (A) Layout of the multicolor 3D QD-LED array design. (B) Schematic showing the QD-LED interconnect assignments, in which the 3D array can be individually controlled via six external contact points. (C) Design schematic of the unit cell of each 3D printed QD-LED. (D) Electroluminescence from three top-layer and three bottom-layer QD-LEDs in the 3D matrix. The six locations (i)–(vi) correspond to the locations indicated by the arrows in panel A. Scale bar is 1 cm.

array of QD-LEDs. Figure 5B shows that the 3D printing-based approach expands the design freedom to a third dimension; enabling the creation of vertical interconnects and stacking of nanoelectronic elements with assignable horizontal and vertical addressing. The construct and material layering of each QD-LED element is shown in Figure 5C, which highlights the integration of seven different materials with diverse properties, enabled by the versatility of our 3D extrusion printing

dx.doi.org/10.1021/nl5033292 | Nano Lett. 2014, 14, 7017–7023

approach. Most importantly, in Figure 5D, we demonstrate the electroluminescence output of multicolor, multidimensionally matrixed 3D printed and embedded QD-LEDs (see Supporting Information for experimental details). The position of each QD-LED element is as indicated in Figure 5A, and panels (i), (ii), and (iii) of Figure 5D exhibit the electroluminescence from three top layer QD-LEDs, whereas (iv), (v), and (vi) show the multicolor electroluminescence from three bottom layer QD-LEDs. We envision that further improvements in printing resolution can lead to a 3D holographic display.

In summary, we demonstrate the 3D printing of interwoven active electronic devices, specifically a QD-LED array in which every component of the device, including the active materials, interconnects, and embedding matrix, is 3D printed. This demonstration represents a proof of concept in combining active nanoelectronic components with the versatility of 3D printing, enabling the three-dimensional freeform fabrication of active electronics. The printed QD-LEDs capture the unique properties of QDs: tunability and pure color emission. Further, combining a complementary 3D light-scanning technique with this approach allows for the fabrication of electronics topographically tailored to curvilinear surfaces. We anticipate that this general strategy can be expanded to 3D print other classes of active devices, such as MEMS devices, transistors, solar cells,[33,74] and photodiodes.[75] Future work will address a number of key challenges. These include (1) increasing the resolution of the 3D printer such that smaller devices can be printed, (2) improving the performance and yield of the printed devices, and (3) incorporating other classes of nanoscale functional building blocks and devices, including semiconductor, plasmonic, and ferroelectric materials. Overall, our results suggest a number of exciting applications, including the generation of geometrically tailored devices containing LEDs and multimodal sensors to provide a new tool for optogenetic studies of neural circuitry.[5] Further, coprinting of active electronics with biological constructs[31] could lead to new bionic devices,[13] such as prosthetic implants that optically stimulate nerve cells.[21]

■ ASSOCIATED CONTENT

Supporting Information

Additional experimental details with materials, methods, and figures. This material is available free of charge via the Internet at http://pubs.acs.org.

■ AUTHOR INFORMATION

Corresponding Author

*E-mail: mcm@princeton.edu. Tel.: (609) 542-0275.

Notes

The authors declare no competing financial interest.

■ ACKNOWLEDGMENTS

We thank Prof. Howard A. Stone, Prof. Barrie S. H. Royce, Prof. Manu S. Mannoor, Prof. Claire F. Gmachl, Prof. Tae-Sik Yoon, Prof. Winston O. Soboyejo, Prof. Craig B. Arnold, Prof. Nan Yao, Dr. Janine Nunes, Wei Ding, Yu Kee Ooi, Barry V. Tassell, Joshua A. Spechler, and Jason Wexler for valuable discussions, equipment support, and technical assistance. M.C.M. acknowledges support of this work by the Defense Advanced Research Projects Agency (No. D12AP00245) and the Air Force Office of Scientific Research (No. FA9550-12-1-0367).

■ REFERENCES

(1) Tian, B. Z.; Cohen-Karni, T.; Qing, Q.; Duan, X. J.; Xie, P.; Lieber, C. M. *Science* **2010**, *329*, 830−834.

(2) Ahn, J. H.; Kim, H. S.; Lee, K. J.; Jeon, S.; Kang, S. J.; Sun, Y. G.; Nuzzo, R. G.; Rogers, J. A. *Science* **2006**, *314*, 1754−1757.

(3) Kim, D. H.; Lu, N.; Ma, R.; Kim, Y. S.; Kim, R. H.; Wang, S.; Wu, J.; Won, S. M.; Tao, H.; Islam, A.; Yu, K. J.; Kim, T. I.; Chowdhury, R.; Ying, M.; Xu, L.; Li, M.; Chung, H. J.; Keum, H.; McCormick, M.; Liu, P.; Zhang, Y. W.; Omenetto, F. G.; Huang, Y.; Coleman, T.; Rogers, J. A. *Science* **2011**, *333*, 838−843.

(4) Ahn, B. Y.; Duoss, E. B.; Motala, M. J.; Guo, X. Y.; Park, S. I.; Xiong, Y. J.; Yoon, J.; Nuzzo, R. G.; Rogers, J. A.; Lewis, J. A. *Science* **2009**, *323*, 1590−1593.

(5) Kim, T.-i.; McCall, J. G.; Jung, Y. H.; Huang, X.; Siuda, E. R.; Li, Y.; Song, J.; Song, Y. M.; Pao, H. A.; Kim, R.-H.; Lu, C.; Lee, S. D.; Song, I.-S.; Shin, G.; Al-Hasani, R.; Kim, S.; Tan, M. P.; Huang, Y.; Omenetto, F. G.; Rogers, J. A.; Bruchas, M. R. *Science* **2013**, *340*, 211−216.

(6) Sekitani, T.; Nakajima, H.; Maeda, H.; Fukushima, T.; Aida, T.; Hata, K.; Someya, T. *Nat. Mater.* **2009**, *8*, 494−499.

(7) Liu, J.; Xie, C.; Dai, X. C.; Jin, L. H.; Zhou, W.; Lieber, C. M. *Proc. Nat. Acad. Sci. U.S.A.* **2013**, *110*, 6694−6699.

(8) Gates, B. D. *Science* **2009**, *323*, 1566−1567.

(9) Nam, S.; Jiang, X. C.; Xiong, Q. H.; Ham, D.; Lieber, C. M. *Proc. Nat. Acad. Sci. U.S.A.* **2009**, *106*, 21035−21038.

(10) Hu, J.; Yu, M. F. *Science* **2010**, *329*, 313−316.

(11) Motoyoshi, M. *Proc. IEEE* **2009**, *97*, 43−48.

(12) Nguyen, T. D.; Deshmukh, N.; Nagarah, J. M.; Kramer, T.; Purohit, P. K.; Berry, M. J.; McAlpine, M. C. *Nat. Nanotechnol.* **2012**, *7*, 587−593.

(13) Mannoor, M. S.; Jiang, Z. W.; James, T.; Kong, Y. L.; Malatesta, K. A.; Soboyejo, W. O.; Verma, N.; Gracias, D. H.; McAlpine, M. C. *Nano Lett.* **2013**, *13*, 2634−2639.

(14) Lewis, J. A. *Adv. Funct. Mater.* **2006**, *16*, 2193−2204.

(15) Adams, J. J.; Duoss, E. B.; Malkowski, T. F.; Motala, M. J.; Ahn, B. Y.; Nuzzo, R. G.; Bernhard, J. T.; Lewis, J. A. *Adv. Mater.* **2011**, *23*, 1335−1340.

(16) Kim, D. H.; Lu, N. S.; Ghaffari, R.; Kim, Y. S.; Lee, S. P.; Xu, L. Z.; Wu, J. A.; Kim, R. H.; Song, J. Z.; Liu, Z. J.; Viventi, J.; de Graff, B.; Elolampi, B.; Mansour, M.; Slepian, M. J.; Hwang, S.; Moss, J. D.; Won, S. M.; Huang, Y. G.; Litt, B.; Rogers, J. A. *Nat. Mater.* **2011**, *10*, 316−323.

(17) Kim, R. H.; Kim, D. H.; Xiao, J. L.; Kim, B. H.; Park, S. I.; Panilaitis, B.; Ghaffari, R.; Yao, J. M.; Li, M.; Liu, Z. J.; Malyarchuk, V.; Kim, D. G.; Le, A. P.; Nuzzo, R. G.; Kaplan, D. L.; Omenetto, F. G.; Huang, Y. G.; Kang, Z.; Rogers, J. A. *Nat. Mater.* **2010**, *9*, 929−937.

(18) Yao, H. F.; Shum, A. J.; Cowan, M.; Lahdesmaki, I.; Parviz, B. A. *Biosens. Bioelectron.* **2011**, *26*, 3290−3296.

(19) Lee, M. S.; Lee, K.; Kim, S. Y.; Lee, H.; Park, J.; Choi, K. H.; Kim, H. K.; Kim, D. G.; Lee, D. Y.; Nam, S.; Park, J. U. *Nano Lett.* **2013**, *13*, 2814−2821.

(20) Xu, L. Z.; Gutbrod, S. R.; Bonifas, A. P.; Su, Y. W.; Sulkin, M. S.; Lu, N. S.; Chung, H. J.; Jang, K. I.; Liu, Z. J.; Ying, M.; Lu, C.; Webb, R. C.; Kim, J. S.; Laughner, J. I.; Cheng, H. Y.; Liu, Y. H.; Ameen, A.; Jeong, J. W.; Kim, G. T.; Huang, Y. G.; Efimov, I. R.; Rogers, J. A. *Nat. Commun.* **2014**, *5*, 3329.

(21) Gossler, C.; Bierbrauer, C.; Moser, R.; Kunzer, M.; Holc, K.; Pletschen, W.; Kohler, K.; Wagner, J.; Schwaerzle, M.; Ruther, P.; Paul, O.; Neef, J.; Keppeler, D.; Hoch, G.; Moser, T.; Schwarz, U. T. *J. Phys. D: Appl. Phys.* **2014**, *47*, 205401.

(22) Mannoor, M. S.; Tao, H.; Clayton, J. D.; Sengupta, A.; Kaplan, D. L.; Naik, R. R.; Verma, N.; Omenetto, F. G.; McAlpine, M. C. *Nat. Commun.* **2012**, *3*, 763.

(23) Tao, H.; Brenckle, M. A.; Yang, M. M.; Zhang, J. D.; Liu, M. K.; Siebert, S. M.; Averitt, R. D.; Mannoor, M. S.; McAlpine, M. C.; Rogers, J. A.; Kaplan, D. L.; Omenetto, F. G. *Adv. Mater.* **2012**, *24*, 1067−1072.

(24) Morin, S. A.; Shevchenko, Y.; Lessing, J.; Kwok, S. W.; Shepherd, R. F.; Stokes, A. A.; Whitesides, G. M. *Adv. Mater.* **2014**, DOI: 10.1002/adma.201401642.
(25) Javey, A.; Nam, S.; Friedman, R. S.; Yan, H.; Lieber, C. M. *Nano Lett.* **2007**, *7*, 773−777.
(26) Gracias, D. H.; Tien, J.; Breen, T. L.; Hsu, C.; Whitesides, G. M. *Science* **2000**, *289*, 1170−1172.
(27) Zheng, W.; Jacobs, H. O. *Adv. Funct. Mater.* **2005**, *15*, 732−738.
(28) Reynolds, K.; O'Riordan, A.; Redmond, G. *Appl. Phys. A Mater. Sci. Process.* **2010**, *98*, 203−209.
(29) Boncheva, M.; Gracias, D. H.; Jacobs, H. O.; Whitesides, G. M. *Proc. Nat. Acad. Sci. U.S.A.* **2002**, *99*, 4937−4940.
(30) Pearce, J. M. *Science* **2012**, *337*, 1303−1304.
(31) Murphy, S. V.; Atala, A. *Nat. Biotechnol.* **2014**, *32*, 773−785.
(32) Malone, E.; Lipson, H. *Rapid Prototyping J.* **2007**, *13*, 245−255.
(33) Sargent, E. H. *Adv. Mater.* **2008**, *20*, 3958−3964.
(34) Symes, M. D.; Kitson, P. J.; Yan, J.; Richmond, C. J.; Cooper, G. J. T.; Bowman, R. W.; Vilbrandt, T.; Cronin, L. *Nat. Chem.* **2012**, *4*, 349−354.
(35) Sun, K.; Wei, T. S.; Ahn, B. Y.; Seo, J. Y.; Dillon, S. J.; Lewis, J. A. *Adv. Mater.* **2013**, *25*, 4539−4543.
(36) Muth, J. T.; Vogt, D. M.; Truby, R. L.; Menguc, Y.; Kolesky, D. B.; Wood, R. J.; Lewis, J. A. *Adv. Mater.* **2014**, DOI: 10.1002/adma.201400334.
(37) Zhao, C.; Wang, C. Y.; Gorkin, R.; Beirne, S.; Shu, K. W.; Wallace, G. G. *Electrochem. Commun.* **2014**, *41*, 20−23.
(38) Lopes, A. J.; MacDonald, E.; Wicker, R. B. *Rapid Prototyping J.* **2012**, *18*, 129−143.
(39) Shirasaki, Y.; Supran, G. J.; Bawendi, M. G.; Bulovic, V. *Nat. Photonics* **2013**, *7*, 13−23.
(40) Gur, I.; Fromer, N. A.; Geier, M. L.; Alivisatos, A. P. *Science* **2005**, *310*, 462−465.
(41) Qian, L.; Zheng, Y.; Xue, J. G.; Holloway, P. H. *Nat. Photonics* **2011**, *5*, 543−548.
(42) Alivisatos, A. P. *Science* **1996**, *271*, 933−937.
(43) Colvin, V. L.; Schlamp, M. C.; Alivisatos, A. P. *Nature* **1994**, *370*, 354−357.
(44) Coe, S.; Woo, W. K.; Bawendi, M.; Bulovic, V. *Nature* **2002**, *420*, 800−803.
(45) Wendel, B.; Rietzel, D.; Kuhnlein, F.; Feulner, R.; Hulder, G.; Schmachtenberg, E. *Macromol. Mater. Eng.* **2008**, *293*, 799−809.
(46) Ladd, C.; So, J. H.; Muth, J.; Dickey, M. D. *Adv. Mater.* **2013**, *25*, 5081−5085.
(47) Dickey, M. D.; Chiechi, R. C.; Larsen, R. J.; Weiss, E. A.; Weitz, D. A.; Whitesides, G. M. *Adv. Funct. Mater.* **2008**, *18*, 1097−1104.
(48) Chiechi, R. C.; Weiss, E. A.; Dickey, M. D.; Whitesides, G. M. *Angew. Chem., Int. Ed.* **2008**, *120*, 148−150.
(49) Anikeeva, P. O.; Halpert, J. E.; Bawendi, M. G.; Bulović, V. *Nano Lett.* **2007**, *7*, 2196−2200.
(50) Chen, O.; Zhao, J.; Chauhan, V. P.; Cui, J.; Wong, C.; Harris, D. K.; Wei, H.; Han, H.-S.; Fukumura, D.; Jain, R. K.; Bawendi, M. G. *Nat. Mater.* **2013**, *12*, 445−451.
(51) Kim, T. H.; Jun, S.; Cho, K. S.; Choi, B. L.; Jang, E. *MRS Bull.* **2013**, *38*, 712−720.
(52) Zhao, J. L.; Bardecker, J. A.; Munro, A. M.; Liu, M. S.; Niu, Y. H.; Ding, I. K.; Luo, J. D.; Chen, B. Q.; Jen, A. K. Y.; Ginger, D. S. *Nano Lett.* **2006**, *6*, 463−467.
(53) Kwak, J.; Bae, W. K.; Lee, D.; Park, I.; Lim, J.; Park, M.; Cho, H.; Woo, H.; Yoon, D. Y.; Char, K.; Lee, S.; Lee, C. *Nano Lett.* **2012**, *12*, 2362−2366.
(54) Lipomi, D. J.; Tee, B. C. K.; Vosgueritchian, M.; Bao, Z. *Adv. Mater.* **2011**, *23*, 1771−1775.
(55) Tan, Z.; Zhang, F.; Zhu, T.; Xu, J.; Wang, A. Y.; Dixon, J. D.; Li, L.; Zhang, Q.; Mohney, S. E.; Ruzyllo, J. *Nano Lett.* **2007**, *7*, 3803−3807.
(56) Haverinen, H. M.; Myllyla, R. A.; Jabbour, G. E. *J. Disp. Technol.* **2010**, *6*, 87−89.
(57) Supran, G. J.; Shirasaki, Y.; Song, K. W.; Caruge, J.-M.; Kazlas, P. T.; Coe-Sullivan, S.; Andrew, T. L.; Bawendi, M. G.; Bulović, V. *MRS Bull.* **2013**, *38*, 703−711.
(58) Hu, H.; Larson, R. G. *J. Phys. Chem. B* **2006**, *110*, 7090−7094.
(59) Deegan, R. D.; Bakajin, O.; Dupont, T. F.; Huber, G.; Nagel, S. R.; Witten, T. A. *Nature* **1997**, *389*, 827−829.
(60) Park, J.; Moon, J. *Langmuir* **2006**, *22*, 3506−3513.
(61) Moffat, J. R.; Sefiane, K.; Shanahan, M. E. R. *J. Phys. Chem. B* **2009**, *113*, 8860−8866.
(62) Shmuylovich, L.; Shen, A. Q.; Stone, H. A. *Langmuir* **2002**, *18*, 3441−3445.
(63) Ouyang, J.; Xu, Q.; Chu, C.-W.; Yang, Y.; Li, G.; Shinar, J. *Polymer* **2004**, *45*, 8443−8450.
(64) Boley, J. W.; White, E. L.; Chiu, G. T. C.; Kramer, R. K. *Adv. Funct. Mater.* **2014**, *24*, 3501−3507.
(65) Wood, V.; Panzer, M. J.; Chen, J.; Bradley, M. S.; Halpert, J. E.; Bawendi, M. G.; Bulović, V. *Adv. Mater.* **2009**, *21*, 2151−2155.
(66) Kim, T. H.; Cho, K. S.; Lee, E. K.; Lee, S. J.; Chae, J.; Kim, J. W.; Kim, D. H.; Kwon, J. Y.; Amaratunga, G.; Lee, S. Y.; Choi, B. L.; Kuk, Y.; Kim, J. M.; Kim, K. *Nat. Photonics* **2011**, *5*, 176−182.
(67) Zhu, T.; Shanmugasundaram, K.; Price, S. C.; Ruzyllo, J.; Zhang, F.; Xu, J.; Mohney, S. E.; Zhang, Q.; Wang, A. Y. *Appl. Phys. Lett.* **2008**, *92*, 023111.
(68) Haverinen, H. M.; Myllyla, R. A.; Jabbour, G. E. *Appl. Phys. Lett.* **2009**, *94*, 073108.
(69) Jarvis, R. A. *IEEE Trans. Pattern Anal. Mach. Intell.* **1983**, *PAMI-5*, 122−139.
(70) Rocchini, C.; Cignoni, P.; Montani, C.; Pingi, P.; Scopigno, R. *Comput. Graphics Forum* **2001**, *20*, 299−308.
(71) Salvi, J.; Pagès, J.; Batlle, J. *Pattern Recognit.* **2004**, *37*, 827−849.
(72) Kim, D. H.; Viventi, J.; Amsden, J. J.; Xiao, J.; Vigeland, L.; Kim, Y. S.; Blanco, J. A.; Panilaitis, B.; Frechette, E. S.; Contreras, D.; Kaplan, D. L.; Omenetto, F. G.; Huang, Y.; Hwang, K. C.; Zakin, M. R.; Litt, B.; Rogers, J. A. *Nat. Mater.* **2010**, *9*, 511−517.
(73) Bandodkar, A. J.; Wang, J. *Trends Biotechnol.* **2014**, *32*, 363−371.
(74) Pattantyus-Abraham, A. G.; Kramer, I. J.; Barkhouse, A. R.; Wang, X. H.; Konstantatos, G.; Debnath, R.; Levina, L.; Raabe, I.; Nazeeruddin, M. K.; Gratzel, M.; Sargent, E. H. *ACS Nano* **2010**, *4*, 3374−3380.
(75) Konstantatos, G.; Howard, I.; Fischer, A.; Hoogland, S.; Clifford, J.; Klem, E.; Levina, L.; Sargent, E. H. *Nature* **2006**, *442*, 180−183.